

Numerical Simulation of FSI Using Combined Fixed Grid and Arbitrary-Lagrangian-Eulerian Method

Mohammed Suleman Aldlemy

Department of Mechanical Engineering, Collage of Mechanical Engineering Technology, Benghazi-Libya
Naser S.Sanoussi

Department of Mechanical Engineering, Collage of Mechanical Engineering Technology, Benghazi-Libya
Saleh S S Elfallah

Department of Mechanical Engineering, Collage of Mechanical Engineering Technology, Benghazi-Libya
Mustafa Agripi Farhat Ahmida

Department of Mechanical Engineering, the Higher Institute for Refrigerating & Air Conditioning – Sokna - Libya

Walid Omar A Salem

Department of Mechanical Engineering, Collage of Mechanical Engineering Technology, Benghazi-Libya
Salah Elbadri

Department of Mechanical Engineering, Collage of Mechanical Engineering Technology, Benghazi-Libya

Abstract - Arbitrary-Lagrangian-Eulerian (ALE) grid methods have shortcomings when it comes to finding solutions to problems undergoing very large deformations. As a result, fixed grid methods have been used to counter these drawbacks. However, the accuracy and precision of fixed grid methods is not as good as when compared with the ALE grid methods. To take advantage of the benefits of both the fixed grid methods and the ALE methods, a combination of the two is paramount. The combinations results into a method that is capable of dealing with complex and large deformations and at the same time, producing results that are accurate and with high precision. The algorithm is then used to simulate 2-D laminar flows past stationary and moving thin structures positioned perpendicular to the freestream direction. The results showed good agreement with those obtained from the ALE algorithm for elastic thin boundaries. It is concluded that the algorithm is capable of predicting the characteristics of laminar flow past an elastic structure with acceptable accuracy with only ~25% of the computational time for simulations.

Index Terms – *FS-Interfaces, ALE, Fixed grid, Numerical Simulation*

INTRODUCTION

The description of laws detailing coupling of dynamics of fluids and structural mechanics is referred to as Fluid-Structure Interactions (FSI) [1], [2]. The phenomenon of FSI entails interaction of fluid flow and a given structure [3]. The movement of the given structure is facilitated by the action of force originating from fluid. The forces induce motions to the structure [4]. The motions are either translational, deformational, rotational or a combination of any of the stated motions [5], [6]. The responses depicted by the structure are as a result of the impact of the fluid. Such impacts include fluid forces, as earlier stated and dynamic forces. Thus, the phenomena of fluid-structure interactions have found numerous applications in aeronautical engineering, biomechanics, wind turbines among other applications [7], [8].

Fluid-structure interaction problems are complex making it difficult to obtain an analytical solution to the problems. Moreover, carrying out experiments to examine and find a solution to given fluid-structure

interaction problem is not always probable due to limited facilities and the high costs involved [9]–[11]. This has resulted in numerical simulations that are aimed at investigating the fundamental physics theories applicable to fluid-structure interaction [5], [12].

This study focuses on a combination of Arbitrary Eulerian Lagrangian benefits and fixed grid approach by use of overlapping grid formulation. In the case, there is an overlapping of the Arbitrary Eulerian Lagrangian on the fixed fluid grid, which is in the background.

A relatively recent development in the computational analysis is a coupling between fluid flow and structural dynamics. These FSIs can be observed in many physical phenomena, including vibrations of the bridge due to gusts, aerodynamic flow patterns in response to flapping, deformation of blood vessels and the heart in response to blood flow and tissue vibrations of the airways in response to breathing during snoring. From the previous studies, two approaches are common in solving FSI (i) Structural mesh that fits the fluid mesh or (ii) structural mesh that does not fit the fluid mesh [10], [13], [14].

In the first (and most common) method, the fluid domain and boundary often change as the interface structure continues to deform [15]. Therefore, the ALE formula is necessary for fluid physics. More importantly, it is necessary to solve the complete meshing or mesh deformation for the entire fluid domain, which involves a lot of calculation work. Or, in the last method where structural grids are not suitable for fluid grids, a fixed fluid grid with Euler's formula for fluid physics is used [12]

This has the advantage of eliminating the need to repeatedly update the fluid domain grid. Several schemes suitable for this method have been developed, including the extended finite element method (XFEM) using Lagrangian multipliers to enhance fluid-structure coupling [13], virtual domain/mortar element method [14], Immersed boundary method (IBM) Use the smooth Dirac-delta function to insert variables between the fluid domain and the structure domain [15], [16] and the submerged finite element method (IFEM). Unlike IBM, the latter uses the method of replicating nuclear particles to insert the interface velocity And physical strength [2].

1.1 Fixed Grid Methods

Fixed grid methods have proven to be efficient in providing solutions to problems that involve large deformation [17]–[19]. The fixed grid method entails a description of the fluid domain using the Eulerian fluid formulation. This does not include deforming fluid meshes and moving fluid meshes. In this regard, fixed grid methods expedite a structure to have a complex and large deformations [11], [20], [21]. In fixed grid methods, there is an independent movement of the structure in the fluid domain. This is an advantage since it allows determination of complex and unlimited deformations on the structure [2]. The description of the FS-interface in the fixed grid approaches is either explicit or implicit. Consequently, the fluid is broken into two sub domains, a fictitious fluid sub – domain and the physical fluid sub – domain [22]. A suitable mesh resolution surrounding a structural surface is paramount in finding solutions to complex FSI problems [17]. This required precision in finding solutions to fluid-structure interactions problems hinders the use of the fixed grid methods, hence the need to develop an effective alternative method. For instance, in the Distributed Lagrange Multiplier method and the Immersed boundary method, (abbreviated as DLM and IBM respectively), there is no production of sharp and accurate representations of the pressure jumps in the FS-interface [23]. Also, the fluid and the structure have a mesh – size dependency. This dependency hinders achievement of an accurate kinematic match between the fluid and the structure [24].

1.2 Arbitrary Eulerian Lagrangian (ALE)

Arbitrary Eulerian Lagrangian (ALE) is an approach that is commonly used to aid in the analysis of the domain motion of the fluid under study [25]. Classically, there is the deformation of the domain onto which the mesh computational domain is discretized. The description of the ALE approach in this paper is based on an assumption that the domain onto which the fluid flows has a boundary that has a definition function. The definition function can be described basing on a body's shape and discretely computed basing on set points [26], [27]. A fluid field in the ALE formulation gives way for finding solutions to the flow field occurring in a grid capable of deforming [8], [28].

The deformable grid undergoes a deformation similar to the structure. This occurs at the interface existing between the solid and the fluid. At the interface, the fluid grid in the dome has arbitrary and extended deformations [29]. This suppresses discretization errors, and it averts distortion of elements.

The ALE methods are advantageous since the various ALE based methods allow theoretical determination of the position of the solid in the fluid domain. This is important because it helps to build a fine mesh close to the surface of the structure so that the flow characteristics around the surface of the structure can be analyzed. The accuracy and precision of the ALE methods are determined by the changes occurring on the size and shape of the subdomains [30]. Small changes results into high accuracy and precision. Large change renders it impossible to maintain mesh distortion leading to deformed mesh that is unusable [28], [31]. The process of eliminating this problem is expensive thus discouraging its use. Also to remedy this, fixed methods can be used. However, fixed methods have their disadvantages as earlier connoted.

1.3 Combined Fixed – ALE.

To eliminate the limits of the fixed grid approach and utilize the advantages of the Arbitrary Eulerian Lagrangian (ALE), a combination of the two (ALE and Fixed grid approach) is essential. The combinations entail finding a solution to the N-S equations by utilizing the Eulerian formulation [32]. The solution to the structural domain is found using the Lagrangian formulation [33]. A boundary layer is then attached to the mesh structure that is then embedded to the background fluid domain. The developed fixed – ALE method can be compute to solve complex FSI problems that are either two or three-dimensional. The combination of the Fixed and ALE methods utilizes the advantages of the two methods in providing the solutions. The definition of the structure in this combination is in Lagrangian formulation. Fluid elements surround the structure. The fluid elements are based on the ALE formulation. The deformation of the fluid patch occurs together with the structure of the boundary layer provided in the simulation [26]. In this method, there is the use of overlapping meshes, though, overlapping solutions are not introduced.

The Euler equations describe compressible inviscid hydrodynamics and can be used to model gas flows, shock reflections and collisions, blast waves, wind tunnel experiments, flow around airfoils, turbulence and many other physical phenomena. Analytical solutions only exist in the simplest cases of geometry, boundary conditions and initial conditions; while physical experiments are often costly, difficult to interpret, affected by additional physics, and time consuming to set up. Computational modelling is often cheaper, faster to set up, allows numerous parameter and geometry studies, and can be used to model situations where a real experiment would be impossible or dangerous. When the Euler equations are discretised on a mesh the solution accuracy will depend on the mesh resolution. Increasing the resolution in areas of the mesh where the solution varies rapidly or over small length scales will increase the solution accuracy. The resolution throughout the domain could be increased, but in realistic models the physical variations or phenomena may be occurring over length scales that are several magnitudes smaller than the domain geometry. Increasing the resolution throughout would require a prohibitively large number of elements and nodes, making the calculation time immense. However, many problems are characterized by features of interest, such as impacts, shear layers, or boundary layers, while the remaining solutions change slowly or stay the same. The practical and efficient approach is to increase the resolution locally around only the features of interest, rather than throughout the entire domain.

Obtaining the resolution required, focusing it in the areas of interest, and keeping the number of nodes and elements to a minimum can be considered to be an optimization problem. There are two main approaches to this optimisation problem: r-refinement where the number of nodes is fixed but they may move to provide higher resolution in specific areas of the domain, or h-refinement where the number of nodes and elements is increased by the subdivision of elements.

The interpolation function that defines the fluid-structure coupling usually blurs or blurs the difference between the FS-interface within the fluid mesh width. In addition, if the boundary layer grid aligned with the structure is not used, it is difficult to capture the resolution of the boundary layer near the surface of the structure.

The adaptive mesh refinement (AMR) approach focuses on the refinement/thickening of certain areas of the mesh according to the dynamic characteristics of the flow to obtain sufficient mesh resolution in any part of the domain and time step of the numerical simulation Rate. The advantage of this method is automatic and

dynamic mesh adaptation to accurately solve the flow problem. Otherwise, the construction of a fixed (static) mesh requires the establishment of a maximum mesh resolution in an area that will not be available at the beginning of the simulation. It is necessary in another simulation time step. In addition to reducing the computational requirements of simulation, it is also important for the algorithm to achieve good parallel performance in today's supercomputers to take advantage of the increasingly available computing power. In this research and for the best knowledge of the authors, a numerical technique is developed based on adaptive mesh refinement integrated with ALE to solve FIS problem

NUMERICAL METHOD

Earlier in the paper, it is stated that the domain onto which the fluid flows is defined by a boundary function. Thus, to find a solution basing on these assumptions, the following algorithm can be used [26], [34]. There is initial updating of the boundary function in the domain onto which the fluid flows.

- I. The mesh is then deformed. The deformation of the mesh is achieved using the ALE concepts
- II. The velocity of the mesh is then calculated
- III. The elements of the finite element are then split
- IV. The resulting unknowns are then computed. The specific instructions on achieving the above instructions is as described below.

Formulation of the Combined Fixed and ALE approach

Solutions to a fluid structure problem to analyze its density and velocity basing on the following conditions;

$$\rho[\partial_t U + (U - U_m) \cdot \nabla U] - \nabla \cdot \sigma = f \quad (1)$$

Where U and ρ velocity and density respectively are, f is the vector representing the body forces and σ represents Cauchy stress tensor.

$$\partial_t \rho + (U - U_m) \cdot \nabla \rho + \rho \nabla \cdot U = 0 \quad (2)$$

In equation 2, the U_m represents the velocity of the ALE system.

Now, consider the domain illustrated below;

$$\Omega(t) \subset \Omega^0 \subset \mathbb{R}^d \quad (3)$$

$\Gamma_{Free}(t)$ is defined using equation 4 below;

$$\Gamma_{Free}(t) = \partial\Omega(t) \cap \partial\Omega^0 \quad (4)$$

Where Γ represents the boundary Meshing Ω^0 with M^0 (FE-mesh) and at a given time t^n meshing Ω^n with M^n (which is FE-mesh). Below is an illustration of mesh deformation

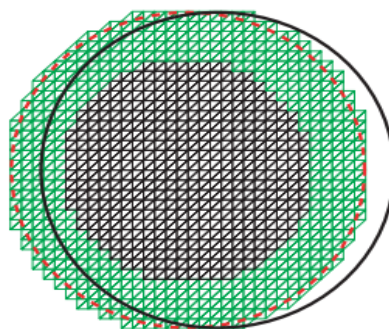


Figure 1: Mesh before deformation i.e. at M^n [34]

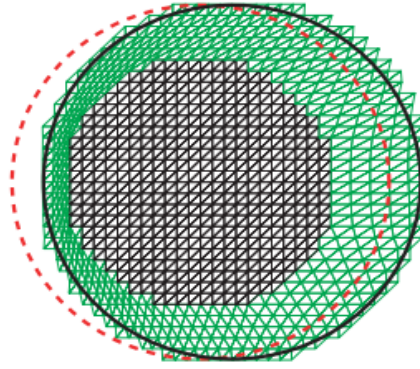


Figure 2: Mesh after deformation i.e. after updating to M_{ALE}^{n+1} [34].

In both figure 1 and figure 2, shows the body surface at t^n . The solid black line show the body surface when the time is at t^{n+1} . From the above diagram, it can be seen that while all the elements are deformed, the darker part remains unreformed. Since U_n is the velocity determined by Ω^n , then Γ_{free}^{n+1} is defined by boundary function updating. The Mesh velocity can then be computed as U_m^{n+1} . Boundary updating entails translation of the domain to Ω^{n+1} from Ω^n [34]. The figure below shows boundary updating

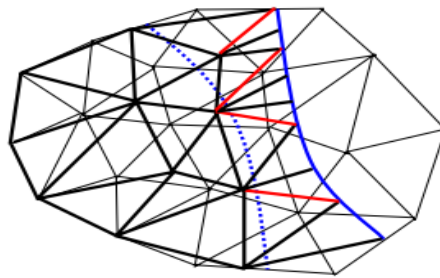


Figure 3: Boundary updating using ALE method.

The blue line shows the new updated position and the previous position is shown by the dotted blue line. The thick black line represents M^n elements while the thin black line represents M^0 elements. The red line shows the transition whereby there is splitting from M^0 to M^n [34].

Using the position of the boundary points (x^{n+1} and x^n), the mesh velocity of the points is determined from the position as shown in the equation 5 and equation 6 below;

$$u_m = (x^{n+1} - x^n) / \partial(t) \quad (5)$$

Determination of U_m on the other nodes is achieved by solving the condition below;

$$\Delta U_m = 0 \quad (6)$$

Using the previously defined domain and the mesh, it is now possible to find the solutions to the following equations.

$$\rho^{n+1} \left[\frac{1}{\delta t} (u^{n+1} - u^n) + (u^{n+1} - u_m) \cdot \nabla U^{n+1} \right] - \nabla \cdot \sigma = f \quad (7)$$

$$\frac{1}{\delta t} (\rho^{n+1} - \rho^n) + (U^{n+1} - U_m) \cdot \nabla \rho^{n+1} + \rho^{n+1} \nabla \cdot U^{n+1} = 0 \quad (8)$$

The solutions to equations 7 and Equation 8 can be determined using the backward Euler scheme. The solutions are based on the boundary conditions Γ_{free}^{n+1} and Ω^{n+1} . This computes the velocity, U_m

Considering the fact that P^{n+1} is a finite element function projection to M^{n+1} from M_{virt}^{n+1} , then the equations on M^{n+1} are as shown by equations 9 and equation 10 below;

$$\rho^{n+1} \left[\frac{1}{\delta t} (u^{n+1} - P^{n+1}(u^n)) + (u^{n+1} - P^{n+1}(u_m)) \cdot \nabla U^{n+1} \right] - \nabla \cdot \sigma = f \quad (9)$$

$$\frac{1}{\delta t} (\rho^{n+1} - P^{n+1}(\rho^n)) + (U^{n+1} - P^{n+1}(U_m)) \cdot \nabla \rho^{n+1} + \rho^{n+1} \nabla \cdot U^{n+1} = 0 \quad (10)$$

Where P^{n+1} corresponds to the finite element projection from M to M^{n+1} . Equation 9 and equation 10 gives the flow equation basing on the combination of the fixed and ALE approach.

SIMULATION RESULTS AND DISCUSSION

This section describes the settings used for 2D laminar flow simulations beyond thin elastic structures. The computational domain has the following dimensions: length \times height = 2.20 m \times 0.41 m. The thin elastic structure is placed in the center of the domain with an axial distance of 1.10 m from the entrance. The height of the thin elastic structure is 0.30 m, and the structure consists of 200 nodes. The Poisson's ratio, Young's modulus, and density of the thin elastic structure are set to 0.30, 5.0 MPa, and 1.0 kg/m³, respectively. Figure 4 shows the geometry of the solution domain, and Table 1 shows the parameters used for fluid flow.

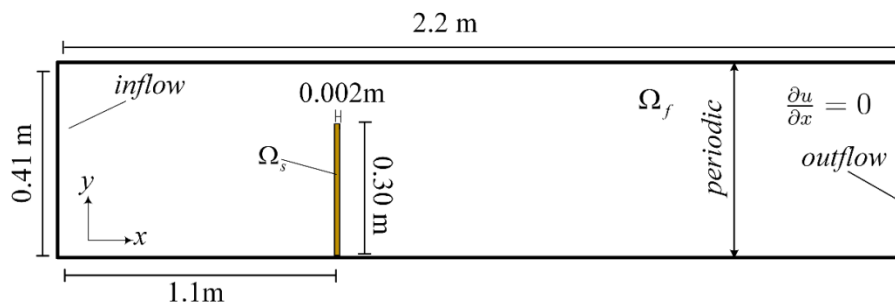


Figure 4: Domain and boundary conditions of two-dimensional thin solid

Table 1: Fluid domain parameters in a 2-D channel

Parameters	Outer Mesh	Refined Mesh Around the Object
Number of nodes	220 \times 41	40 \times 240
Re $\bar{U}D=\rho$	20	20
Increment of Time, Δt	5×10^{-3}	6.25×10^{-6}
Grid size, $\Delta x, \Delta y$	0.01	0.00125
Free stream velocity U_o	0.3	0.3

The following screenshots shows simulation in ANSYS Simulation Software. This simulation shows the flow of a fluid around a cantilever. The figure 5 indicates velocities and pressure of the fluid at 100-time step. Figure 5 shows the pressure and velocity profiles of the laminar flow around the static thin structure. It can be seen that the flow velocity is usually higher than the structure, starting from the middle of the structure, as indicated by the yellow, orange and red regions. Interestingly, the flow will decelerate in front of the body, while the flow velocity behind the body is still very low, as shown in the highlighted blue region in Figure 5. The pressure before the thin structure is much higher, as shown in the red region, and the pressure drops abruptly after passing fluid through the body. Displacement time graph obtained from the data is as shown below;

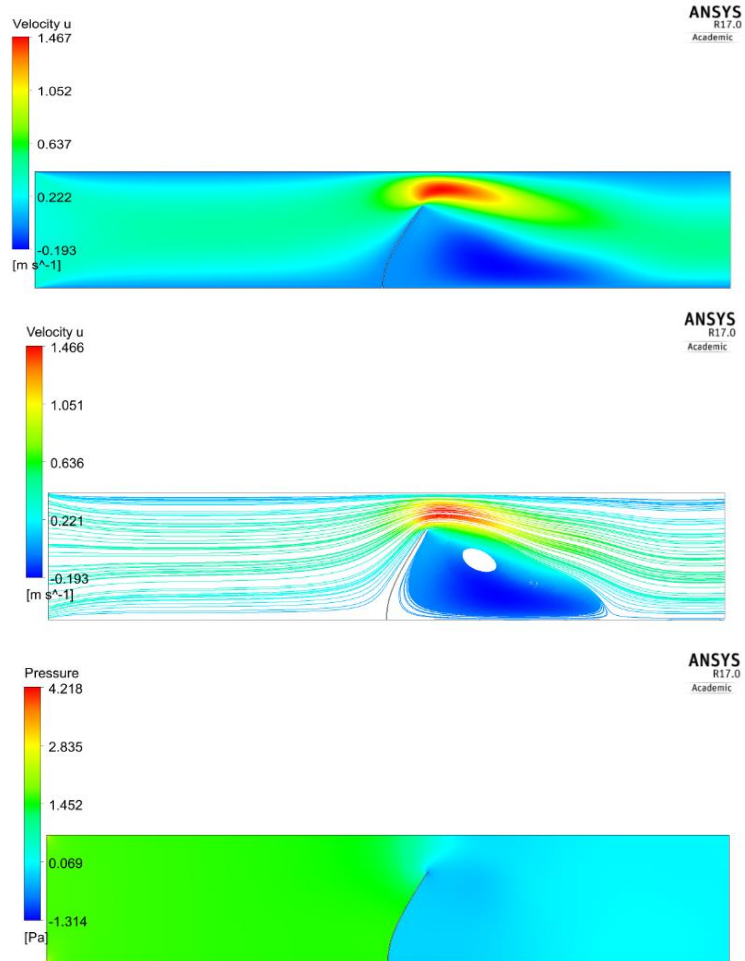


Figure 5: Simulation Fluid flow around a cantilever used Purely ALE method

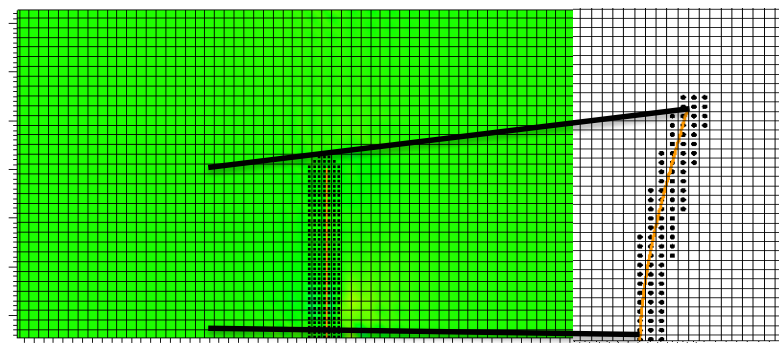


Figure 6 Snapshots the deformed immersed thin structure and fixed background fluid mesh with refinement mesh around of the thin elastic structure and a boundary layer of mesh.

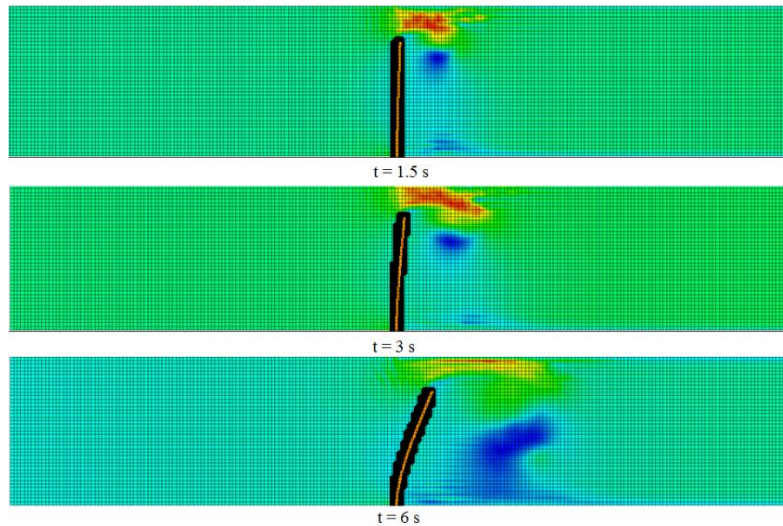


Figure 7: Simulation Fluid flow around a cantilever used the combined fixed and ALE method

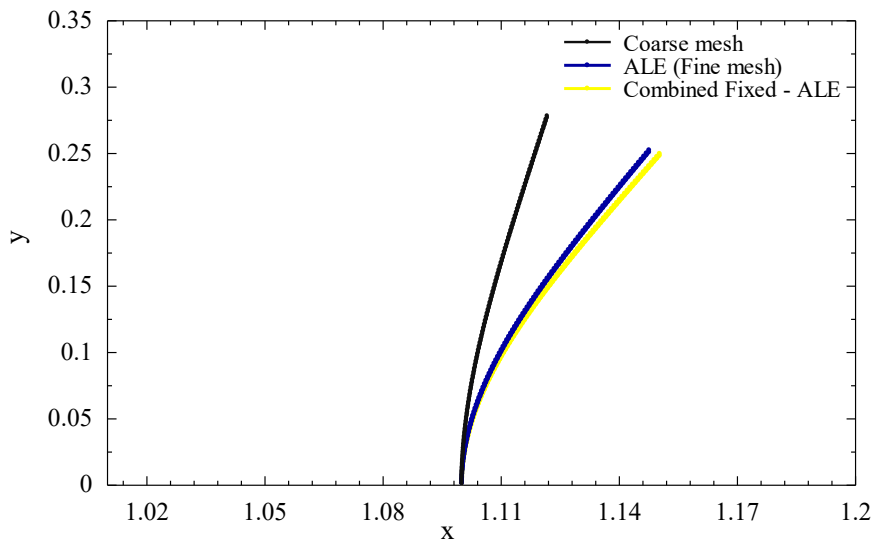


Figure 8: Graph showing Horizontal displacement vs. time step during simulation

Figure 8 shows a plot in indicating how a point that has been placed on top of the cantilever has been displaced horizontally. On examination of this figure, it can be seen that the fluid's action damps the cantilever's movement. The movement increases from the start and after some time, it becomes almost constant. . The main feature of this locally refined mesh surrounding the object is its dynamic movement, which does not require much computation as the determination is limited and does not include the entire domain space

In the above simulation, the body in the fluid experiences very large strains due to the force resulting from the fluid flow. As earlier stated, ALE grid methods are not efficient in such scenarios due to the large element stretch. However, it's been possible to get accurate and robust results as shown due to the fact that, the combined method has aided in the aversion of stretching of the elements by the use of the fixed grid method properties. Re-meshing has been avoided, as it would have been done in the classical ALE methods.

Generally, the use of the combined methods make it easy to mesh the background domain, and the avoidance of mesh distortion when dealing with large deformations. Figure 7 show velocity in x direction after 0.453 seconds. Figure 5 shows simulation results when using pure ALE method and figure 7 shows results when using Combined fixed – ALE method. It can be seen that due to the very high deformation of the mesh, of the purely ALE approach after a given time. This is contrary to when there is the use of combined fixed – ALE method.

Figure 9: shows is an illustration mesh size of combined Fixed – ALE of the fluid interaction. The mesh size near the thin elastic structure must be fine enough to accurately capture the flow physics at the FS-interface. The fixed and ALE combined method is used to locally adjust and refine the fluid mesh size near the limit of the thin elastic structure, without the need to refine the entire calculation domain, so this method is more efficient. The fluid element and the solid node are attached to the boundary without any discontinuity, and can capture any deformation of the thin elastic structure. The surface integral at the FS- interface is considered massless and can be eliminated when the stiffness matrix is formed. This processing eliminates the need to calculate surface forces at the FS-interface.

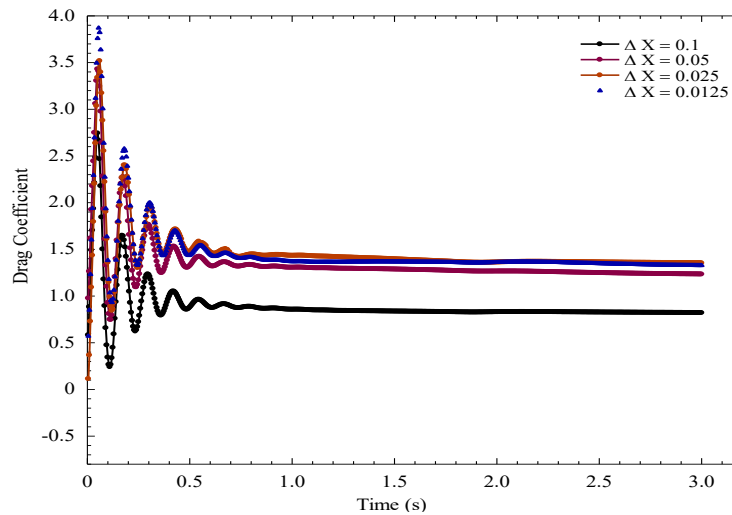


Figure 9: shows is an illustration mesh size of combined Fixed – ALE of the fluid interaction.

Figure 10 shows the comparison of the **Cd** values obtained from the combined fixed ALE and pure ALE. The **Cd** value is determined by the simulation result of the combined fixed ALE, and the value is compared with the result obtained from the pure ALE method. Use ANSYS 17.0 software. The direction here is the total hydrodynamic force. Figure 10 shows the difference of the **Cd** of the deformed thin elastic structure valve over time. These changes are obtained from a combination of fixed ALE and pure ALE algorithms with the same mesh size and initial time step. The error of the **Cd** is very small (estimated at ~2%), indicating that the values of the Cd between the algorithms have good consistency. However, from a computational point of view, the fixed ALE combination algorithm is much simpler to implement and relatively cheap.

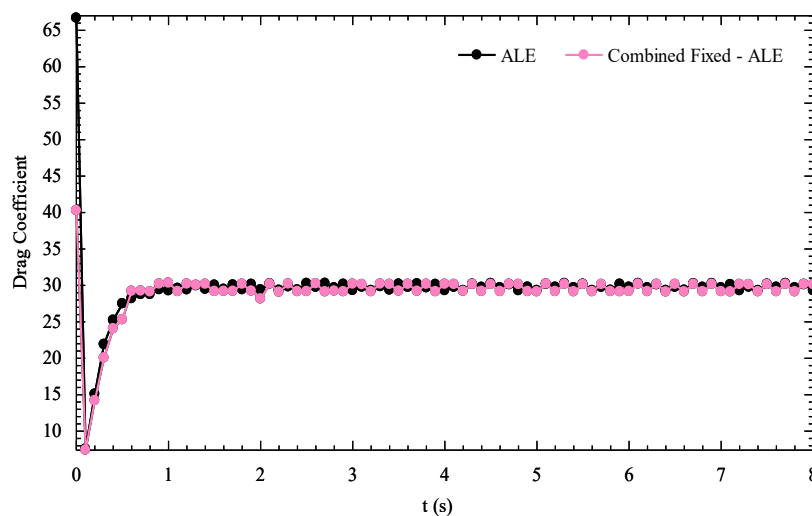


Figure 10: Comparison of drag coefficient values obtained by combining Fixed-ALE and pure ALE algorithms

CONCLUSION

The main purpose of this research is to develop an algorithm based on a fixed grid combined with arbitrary-Lagrangian-Euler Method to improve the simulation solution of the FSI problem of thin objects near the fluid-structure interface. The study illustrates the benefits of using ALE-based FSI methods and fixed complex technology. The combination of these two techniques facilitates the analysis of complex FSI problems that experience large deformations. Next, the algorithm is calculated to simulate the laminar flow outside the fixed and moving thin structures representing the membrane valve in the two-dimensional domain. According to the combined result, it can be seen that the background is easier to be gridded, and there is no grid distortion. Compared with soft computing modeling, modeling is simple and less time-consuming. It can be extended to new areas that require higher resolution or rely on the parallel scaling properties of the solver.

REFERENCES

- [1] M. P. Paidoussis, *Fluid-structure interactions: slender structures and axial flow*, vol. 1. Academic press, 1998.
- [2] H.-J. Bungartz and M. Schäfer, *Fluid-structure interaction: modelling, simulation, optimisation*, vol. 53. Springer Science & Business Media, 2006.
- [3] A. M. S. Al-Janabi, A. H. Ghazali, Y. M. Ghazaw, H. A. Afan, N. Al-Ansari, and Z. M. Yaseen, "Experimental and numerical analysis for earth-fill dam seepage," *Sustain.*, 2020.
- [4] N. S. Radhi, K. F. Morad, M. H. Hafiz, A. A. Atiyah, and A. Bouaissi, "OPTIMIZATION OF NICKEL CONTENT ON SOME PROPERTIES OF (NITI) SHAPE MEMORY ALLOY," *Knowledge-Based Eng. Sci.*, vol. 1, no. 1, pp. 40–47, 2020.
- [5] C. H. Tai, K. M. Liew, and Y. Zhao, "Numerical simulation of 3D fluid–structure interaction flow using an immersed object method with overlapping grids," *Comput. Struct.*, vol. 85, no. 11–14, pp. 749–762, Jun. 2007.
- [6] S. Q. Salih *et al.*, "Thin and sharp edges bodies–fluid interaction simulation using cut-cell immersed boundary method," *Eng. Appl. Comput. Fluid Mech.*, vol. 13, no. 1, pp. 860–877, 2019.
- [7] T. T. Nguyen, D. Shyam Sundar, K. S. Yeo, and T. T. Lim, "Modeling and analysis of insect-like flexible wings at low Reynolds number," *J. Fluids Struct.*, vol. 62, pp. 294–317, 2016.
- [8] M. R. Rasani, M. S. Aldlemy, and Z. Harun, "Fluid-structure interaction analysis of rear spoiler vibration for energy harvesting potential," *J. Mech. Eng. Sci.*, vol. 11, no. 1, pp. 2415–2427, 2017.
- [9] B. Sebastian, T. Dunne, and R. Rannacher, "Numerics of Fluid-Structure Interaction," vol. 37, pp. 333–378, 2008.
- [10] M. S. Aldlemy, M. R. Rasani, A. K. Ariffin, and T. M. Y. S. T. Ya, "Adaptive mesh refinement immersed boundary method for simulations of laminar flows past a moving thin elastic structure *," vol. 32, no. 1, pp. 148–160, 2020.
- [11] M. S. Aldlemy, M. Rasani, T. M. Y. S. Ya, and A. K. Ariffin, "Dynamic adaptive mesh refinement of fluid structure interaction using immersed boundary method with two stage corrections," *Sci. Iran.*, p. , 2018.
- [12] O. A. Alawi *et al.*, "Effects of binary hybrid nanofluid on heat transfer and fluid flow in a triangular-corrugated channel: An experimental and numerical study," *Powder Technol.*, 2022.
- [13] W. A. Wall, A. Gerstenberger, P. Gammitzer, C. Förster, and E. Ramm, "Large deformation fluid-structure interaction--advances in ALE methods and new fixed grid approaches," in *Fluid-structure interaction*, Springer, 2006, pp. 195–232.
- [14] G. Hou, J. Wang, and A. Layton, "Numerical Methods for Fluid-Structure Interaction — A Review," vol. 12, no. 2, pp. 337–377, 2012.
- [15] M. Aldlemy, "EFFECT OF CONDUCTIVITY IN CORROSION PROBLEM USING BOUNDARY ELEMENT METHOD AND GENETIC ALGORITHM," *Knowledge-Based Eng. Sci.*, vol. 1, no. 01, pp. 58–63, 2020.

- [16] M. B. Ghomizad, H. Kor, and K. Fukagata, “A structured adaptive mesh refinement strategy with a sharp interface direct-forcing immersed boundary method for moving boundary problems,” vol. 16, no. 2, pp. 1–22, 2021.
- [17] W. Wall, A. Gerstenberger, and U. Mayer, “Advances in fixed-grid fluid structure interaction,” in *ECCOMAS Multidisciplinary Jubilee Symposium*, 2009, pp. 235–249.
- [18] O. A. Alawi, A. H. Abdelrazek, M. S. Aldlemy, and W. Ahmed, “Heat Transfer and Hydrodynamic Properties Using Different Metal-Oxide Nanostructures in Horizontal Concentric Annular Tube : An Optimization Study,” 2021.
- [19] R. S. Mohammad, M. S. Aldlemy, S. Al Hassan, A. I. Abdulla, M. Scholz, and Z. M. Yaseen, “Frictional Pressure Drop and Cost Savings for Graphene Nanoplatelets Nanofluids in Turbulent Flow Environments,” pp. 1–17, 2021.
- [20] M. M. A. Campos *et al.*, “Determination of lead content in medicinal plants by pre-concentration flow injection analysis--flame atomic absorption spectrometry,” *Phytochem. Anal. An Int. J. Plant Chem. Biochem. Tech.*, vol. 20, no. 6, pp. 445–449, 2009.
- [21] M. S. Aldlemy, M. R. Rasani, T. M. Y. S. Tuan, and A. K. Ari, “Dynamic adaptive mesh refinement of fluid-structure interaction using immersed boundary method with two-stage corrections,” vol. 26, pp. 2827–2838, 2019.
- [22] T. Lee, M. Leok, and N. H. McClamroch, “Geometric numerical integration for complex dynamics of tethered spacecraft,” *Proc. 2011 Am. Control Conf.*, no. April, pp. 1885–1891, 2011.
- [23] H.-J. Bungartz, M. Mehl, and M. Schäfer, *Fluid Structure Interaction II: Modelling, Simulation, Optimization*, vol. 73. Springer Science & Business Media, 2010.
- [24] T. Dunne, R. Rannacher, and T. Richter, “Numerical simulation of fluid-structure interaction based on monolithic variational formulations,” *Fundam. trends fluid-structure Interact.*, pp. 1–75, 2010.
- [25] C. Farhat and V. K. Lakshminarayan, “An ALE formulation of embedded boundary methods for tracking boundary layers in turbulent fluid–structure interaction problems,” *J. Comput. Phys.*, vol. 263, pp. 53–70, Apr. 2014.
- [26] R. Codina, G. Houzeaux, H. Coppola-Owen, and J. Baiges, “The fixed-mesh ALE approach for the numerical approximation of flows in moving domains,” *J. Comput. Phys.*, vol. 228, no. 5, pp. 1591–1611, 2009.
- [27] S. Liu, H. A. Afan, M. S. Aldlemy, N. Al-Ansari, and Z. M. Yaseen, “Energy analysis using carbon and metallic oxides-based nanomaterials inside a solar collector,” *Energy Reports*, vol. 6, pp. 1373–1381, 2020.
- [28] C. Soullaine, M. Quintard, B. Baudouy, and R. Van Weelderren, “Numerical Investigation of Thermal Counterflow of He II Past Cylinders,” *Phys. Rev. Lett.*, vol. 118, no. 7, pp. 1–5, 2017.
- [29] T. Wick, “Flapping and contact FSI computations with the fluid-solid interface-tracking/interface-capturing technique and mesh adaptivity,” *Comput. Mech.*, vol. 53, no. 1, pp. 29–43, 2014.
- [30] J. Donea, A. Huerta, and J. Ponthot, “Ph., Rodriguez-Ferran A. Arbitrary Lagrangian-Eulerian methods. Encyclopedia of computational mechanics,” *Fundamentals*, vol. 1, 2004.
- [31] M. S. Aldlemy, S. A. K. A. R. A. M. A. T. Ya, and R. Alebrahim, “Composite patch reinforcement of a cracked simply-supported beam traversed by moving mass,” vol. 14, no. 1, pp. 6403–6416, 2020.
- [32] S. Shahmiri, “A Hybrid ALE-Fixed-Grid Approach for Fluid-Structure Interaction,” vol. 22, no. 22, 2014.
- [33] X. YANG and M. bin LIU, “Bending modes and transition criteria for a flexible fiber in viscous flows,” *J. Hydrodyn.*, vol. 28, no. 6, pp. 1043–1048, 2016.
- [34] J. Baiges Aznar, “The Fixed-Mesh ALE method applied to multiphysics problems using stabilized formulations,” *Mater.*, vol. 14, no. December, pp. 01–2011, 2011.